Novel Miscible Polymer Blend of Poly(4-trimethylsilylstyrene) and Polyisoprene

Masashi Harada,*,†,‡ Takahisa Suzuki,†,§ Masayuki Ohya,† Daisuke Kawaguchi,† Atsushi Takano,† and Yushu Matsushita*,†

Department of Applied Chemistry, Nagoya University, Nagoya, Aichi 464-8603, Japan, and Toyota Central R&D Laboratories, Inc., Nagakute-cho, Aichi 480-1192, Japan

Received July 19, 2004; Revised Manuscript Received October 26, 2004

ABSTRACT: The phase behavior of the newly found miscible polymer blends poly(4-trimethylsilylstyrene) and polyisoprene was investigated with optical microscopy (OM) and also with differential scanning calorimetry (DSC), while the degree of polymer−polymer interaction was evaluated with small-angle neutron scattering (SANS). The blends with homogeneous one phase at various compositions turned into two phases by heating, showing a lower critical solution temperature (LCST) type phase diagram with a critical temperature of 172 °C if the degree of polymerization is ca. 370. The blend gave a single glass transition temperature below the LCST, and the interaction parameter χ was represented as a function of temperature T according to the relationship $\chi = 0.027 - 9.5/T$.

Introduction

Multicomponent polymer systems have been a target of experimental and theoretical studies for understanding phase behavior and morphology.[1] Many researchers were attracted by the diverse phase diagram displayed by polymer blends[2,3] and block copolymers,[4,5] which is governed by the complex interaction between component polymers. Polymer blends favors the immiscible state from little gain of entropy of mixing; however, some miscible polymer blends were discovered[6,7] and were applied to design simple polymer alloys with intermediate properties of each component. Although polystyrene/poly(vinyl methyl ether) blend may be the most familiar and well-investigated system as miscible polymer blends,[8] studies at the molecular level have been limited by the potential of designing molecular structures of poly(vinyl methyl ether). Anionic polymerization has been the most sophisticated technique to design polymer molecules; that is, the molecular weight can be precisely controlled by this method, and many interesting polymer architectures have been realized. Therefore, the miscible polymer pair, both of which can be synthesized anionically, is a desirable system to study phase behavior accurately.

4-Trimethylsilylstyrene[9] and isoprene have known to be polymerized anionically to give monodisperse polymers. Although no attractive interaction between those polymers was expected, we found with serendipity that poly(4-trimethylsilylstyrene) (PTMSS) and polyisoprene (PI) composed of 1,2- and 3,4-microstructure dominantly showed one phase for a star-shaped tetrablock copolymer by transmission electron microscopy (TEM). PTMSS has a bulky functional group with silicon and has been studied for application to such as separation membranes[10] and bilayer resists[11] because it has high permeability to gases and high durability against O_2-plasma etching. 1,2- and 3,4-rich PI is quite stable since it has double bonds as a side chain, compared with *cis*-1,4 PI which is well-known as a resource of natural rubber. Thus, the blends of PTMSS/PI are expected to develop high-performance materials.

To elucidate that PTMSS and PI are miscible at the molecular level, the phase behavior of the blends is investigated with optical microscopy (OM) and with differential scanning calorimetry (DSC), while the polymer−polymer interaction is evaluated by small-angle neutron scattering (SANS) in this work.

Experimental Section

Preparation and Characterization of Polymer Samples. 4-Trimethylsilylstyrene and the partially deuterated 4-trimethylsilylstyrene-d_9 monomers were prepared by the reaction of Grignard reagent derived from 4-chlorostyrene (Hokko Chemical Industry) with chlorotrimethylsilylsilane (Aldrich) and the chlorotrimethylsilylsilane-d_9 (CDN Isotopes), respectively. The details of monomer synthesis were reported in a previous paper.[12]

Poly(4-trimethylsilylstyrene) (PTMSS) and the deuterated counterpart (*d*-PTMSS) were synthesized by anionic polymerization in THF at −78 °C, which is initiated with *sec*-butyllithium and quenched with 2-propanol, in sealed glass reactors with break-seals under high vacuum. Polyisoprene (PI) was also synthesized in almost the same manner using cumyl potassium as an initiator. Preparation and purification methods were described elsewhere.[12] Tacticity of PTMSS and microstructure of PI were investigated by ^{13}C NMR at 126 MHz and ^{1}H NMR at 500 MHz, respectively, with a Unity Inova 500 of Varian Inc. in $CDCl_3$ at room temperature. Chemical shifts were referred to residual $CHCl_3$ in $CDCl_3$.

Molecular weights were determined by multiangle laser light scattering (MALLS) using a DAWN EOS of Wyatt Technology Inc. at 35 °C in THF with d*n*/d*c* of 0.143, 0.138, and 0.126 for PTMSS, *d*-PTMSS, and PI, respectively. The molecular weight distribution was estimated with gel permeation chromatography (GPC) using a set of three G4000H$_{HR}$ columns of Tosoh Ltd. at 38 °C with THF as an eluting solvent at a flow rate of 1 mL/min. Densities of polymers were measured with the gas displacement technique using helium gas at 10 psi on an Ultra pycnometer 1000 of Quantachrome Co.

Miscibility Measurements. The phase diagram was determined with optical microscopy (OM) using a BH2 of

---

† Nagoya University.

‡ Toyota Central R&D Laboratories, Inc.

§ Present address: JSR, Co.

* Corresponding author: e-mail harada@mosk.tytlabs.co.jp.

10.1021/ma048527+ CCC: $30.25

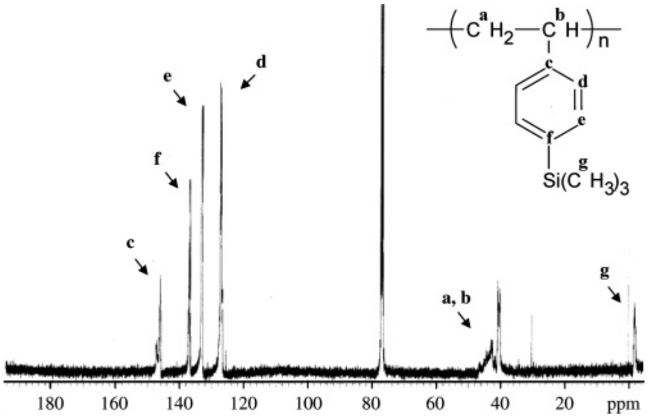

Figure 1. ^{13}C NMR chart of PTMSS. Each peak is assigned to the carbon indicated in the inset.

Olympus equipped with a temperature controller FP82 of Mettler. The samples were cast on coverglasses from 5 wt % solution in THF and annealed at 150 °C for several days. The measurement was performed at a heating rate of 1 °C/min under a nitrogen atmosphere.

The glass transition temperature (T_g) was measured with differential scanning calorimetry (DSC) using a Q1000 of TA Instruments Inc. The sample films were obtained by solution-cast and were annealed at 150 °C under vacuum for several days. The measurements were performed at a heating rate of 10 °C/min after heating for 1 h and quenching to −50 °C under a nitrogen atmosphere. T_g was estimated from the midpoint of the heat capacity jump.

Measurements of Small-Angle Neutron Scattering. Small-angle neutron scattering (SANS) was measured using the SANS-U spectrometer of the Institute for Solid State Physics, the University of Tokyo installed at JRR-3M of Japan Atomic Energy Research Institute in Tokai, Japan. Blend films were prepared by casting from toluene solutions of *d*-PTMSS and PI for several days. Dried films were set in quartz cells with 1.5 mm thickness and were annealed at 170 °C, followed by sealing under high vacuum. SANS measurements were carried out for 0.5 h each at the various temperatures from 145 to 195 °C. The wavelength of the neutron beam was 0.7 nm, the sample-to-detector distance was held at 2 m, and the pinhole with 3 mm in diameter was set just upstream of samples. The SANS intensities were counted on the 2D-PSD and averaged circularly. Incoherent scattering intensities were estimated from the intensities for normal hydrogenated poly(4-trimethylsilylstyrene) measured under the same conditions assuming additivity of volume.[13] The absolute intensities were obtained with the Lupolene standard which has been already calibrated.[14]

Results and Discussion

The tacticity of PTMSS and the microstructures of PI are investigated to elucidate the phase behavior of the blends rigorously, since it is known that tacticity[15] and microstructures[16] have effects on polymer blend miscibility. Figure 1 shows the ^{13}C NMR chart of PTMSS prepared by the above-mentioned procedures. The spectra around 147 ppm are derived from the aromatic C-1 carbon, c, showing multipeaks which can be assigned to isotactic, heterotactic, and syndiotactic triads.[17] If the polymers were isotactic or syndiotactic, the single peak should be observed; therefore, we are convinced that the PTMSS is atactic. Figure 2 shows the ^{1}H NMR chart of PI prepared by the above-mentioned procedures. The signal around 5.8 ppm is derived from the protons at the 3-position of 1,2-microstructure, the signal around 4.7 ppm is derived from the protons at the 4-position of 1,2-microstructure, 1-position of 3,4-microstructure and 3-position of 1,4-microstructure, and the signal around 2.0 ppm is derived from the protons at the 3-position of 3,4-microstructure and 1-position and 4-position of 1,4-microstructure.[18] From the intensity ratio the microstructure ratio of 1,2-microstructure:3,4-microstructure:1,4-microstructure is evaluated as 46:48:6, in contrast to the natural rubber having almost 100% 1,4-microstructure.

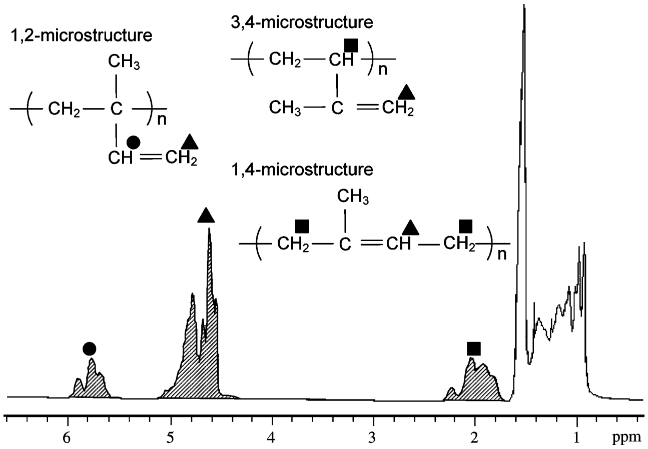

Figure 2. ^{1}H NMR chart of PI. Characteristic peaks to identify the microstructures are hatched, and the corresponding protons are presented with marks in the insets.

Table 1. Molecular Characteristics

code	polymer	$M_w{}^a$ (g/mol)	$M_w/M_n{}^b$	ρ^c (g/cm^3)
blend-s	PTMSS	35 000	1.02	0.963
	d-PTMSS	33 800	1.02	1.006
	PI	11 100	1.07	0.926
blend-l	PTMSS	68 000	1.01	0.963
	d-PTMSS	70 000	1.03	1.006
	PI	25 000	1.05	0.926

[a] Weight-average molecular weights measured by MALLS. [b] Polydispersity indices measured by GPC. [c] Densities estimated with the gas displacement technique.

The molecular characteristics of PTMSS, *d*-PTMSS, and PI are given in Table 1. Two sets of polymers with different molecular weight, blend-s and blend-l, are employed in this study. The molecular weight of PTMSS is pretty close to that of *d*-PTMSS, and both of them were prepared under controlled conditions so as to match their degree of polymerization with those of the corresponding PI. The density increase of *d*-PTMSS against PTMSS is consistent with the molecular weight increase by deuterium labeling, while the density of PTMSS is larger than that of PI.

Blend-s with various PTMSS volume fractions from 0.09 to 0.89 were observed by OM. All of the blends were homogeneous and looked transparent in a temperature range from 150 to 240 °C, suggesting miscibility of PTMSS/PI blends.

To examine miscibility of PTMSS/PI blends, T_g's of blend-s with the PTMSS volume fraction of 0.48 were measured by DSC at different annealing temperature from 150 to 240 °C. Their thermograms are shown in Figure 3. A broad single T_g around 25 °C was observed for all blends, and hence miscibility is evident. Then T_g's of blend-s annealed at 150 °C was measured by DSC with PTMSS volume fraction varied. A single T_g was observed for all blends, and the data obtained are plotted in Figure 4. It is apparent that the T_g increases monotonically with increasing PTMSS fraction from the value of PI homopolymer, i.e. 10 °C to that of PTMSS

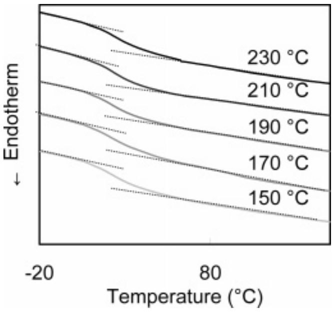

Figure 3. Thermograms of blend-s annealed at various temperatures. The volume fraction of PTMSS is 0.48. Each line is shifted for clarity. Dotted lines are drawn as a guide for the eyes.

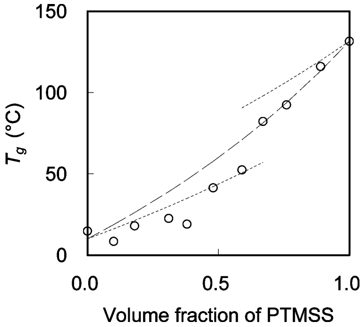

Figure 4. Composition dependence of glass transition temperature for blend-s. The blends are annealed at 150 °C. The broken line denotes the Fox equation, while the dotted lines expresses the self-concentration theory.

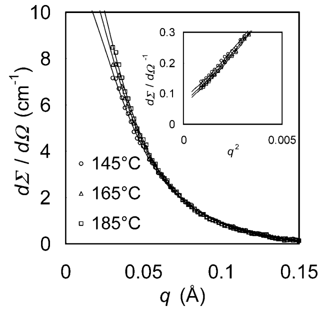

Figure 5. SANS profiles of blend-s heated from 145 °C. The volume fraction of PTMSS is 0.45. The lines are the fitting results with eq 1. The fitting parameters are listed in Table 2. The inlet figure at upper right includes the Zimm plots of the data.

homopolymer, i.e. 135 °C. A particularly sharp increase is observed when the volume fraction of PTMSS exceeds 0.5. While the Fox equation[19] overlaid in Figure 4 with the dotted lines is a good estimate for the behavior, the self-concentration theory[20] overlaid in Figure 4 with the broken line provides a better explanation, especially for the blends with low PTMSS volume fraction. It is interesting to know that at room temperature the PTMSS/PI blends change continuously from rubbery state to glassy one depending on compositions.

The phase behavior of the *d*-PTMSS/PI blend of blend-s was investigated by SANS measurements. *d*-PTMSS instead of PTMSS is employed to earn the contrast against PI, providing negligible effects of deuterium labeling,[21] which could be supported by the small interaction parameter of isotope blends.[22] The SANS profiles of the *d*-PTMSS/PI blends measured at three different temperatures are shown in Figure 5. The intensities in the low-q regime increase slightly as the blends are heated, indicating the growth of the concentration fluctuation induced by the repulsive interaction between component polymers. The same result is obtained by the Zimm plots inserted in Figure 5, which show the shift-down of the line as the temperature increase.

Table 2. Fitting Parameters

code	polymer	a^a (fm)	v^b (nm^3)	ϕ^c	N^d	$R_g{}^e$ (Å)
blend-s	*d*-PTMSS	111	0.305	0.452	183	40.5
	PI	3.33	0.122	0.548	163	31.3
blend-l	*d*-PTMSS	111	0.305	0.479	380	58.3
	PI	3.33	0.122	0.521	363	46.7

[a] Scattering lengths per monomer. [b] Volumes per monomer. [c] Volume fractions in blends. [d] Degrees of polymerization. [e] Radii of gyration for polymers.

The SANS data are analyzed using the equation based on the random phase approximation (RPA) for miscible blends[23] according to eq 1

$$\frac{\mathrm{d}\Sigma}{\mathrm{d}\Omega} = \left(\frac{a_\mathrm{A}}{v_\mathrm{A}} - \frac{a_\mathrm{B}}{v_\mathrm{B}}\right)^2 \Bigg/ \left[\frac{1}{\phi_\mathrm{A} N_\mathrm{A} v_\mathrm{A} P_\mathrm{A}(q)} + \frac{1}{\phi_\mathrm{B} N_\mathrm{B} v_\mathrm{B} P_\mathrm{B}(q)} - 2\,\frac{\chi}{v_0}\right] \quad (1)$$

where a_i is the scattering length per monomer, ν_i is the volume per monomer, ϕ_i is the volume fraction, N_i is the polymerization index, and $P_i(q)$ is the particle scattering function of the polymer component i (= A or B), while v_0 is the reference volume and χ denotes the Flory−Huggins parameter of the segmental interaction. a_i, ν_i, ϕ_i, and N_i are calculated with the scattering lengths of the component atoms, bulk densities, weight fractions, and molecular weights, respectively. It should be noted that bulk densities are a function of the temperature. However, we employed a constant value measured at room temperature since monomer volume change affects less than several percent for temperature change from room temperature to the measurement temperatures due to the small expansion coefficient of polymers.[24]

The Debye function is employed to represent the scattering factor of a single chain;[25] it can be expressed as

$$P_i(q) = \frac{2}{(R_{\mathrm{g},i}{}^2 q^2)^2}[\exp(-R_{\mathrm{g},i}{}^2 q^2) + R_{\mathrm{g},i}{}^2 q^2 - 1] \quad (2)$$

where $R_{g,i}$ is the radius of gyration of the component i. R_g of PTMSS was obtained from the SANS measurements for *d*-PTMSS/PTMSS blends at 150 °C,[12] which is consistent with the value obtained from intrinsic viscosity measurements.[26] R_g of PI was estimated from the intrinsic viscosity measurements of PI in the θ solvent of 1,4-dioxane at the θ temperature of 36.3 °C, which agrees with the reported value.[27] All the parameters determined by the fitting are listed in Table 2. The reference volume v_0 is defined as $(v_\mathrm{A}v_\mathrm{B})^{1/2}$ and is estimated to be 0.193 nm^3. Although R_g should also be a function of temperature, we set it constant because it is known that R_g show small change on temperature[28] whether the polymers are in a θ solvent or in bulk.[29]

To evaluate the interaction parameter χ, the least-squares fittings with eq 1 were performed to the SANS data, where χ was set as a fitting parameter and a baseline factor was introduced to adjust insufficient data

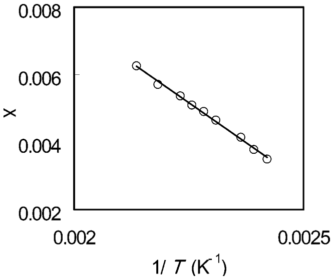

Figure 6. Temperature dependence for χ parameter of blend-s. The line is a least-squares linear fitting result.

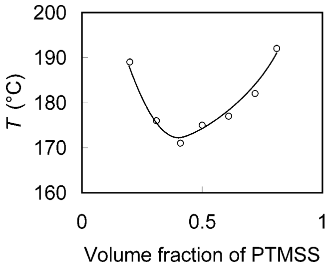

Figure 7. Phase diagram of blend-l. The line is drawn as a guide for the eyes.

correction for absolute coherent scattering cross section. As overlaid in Figure 5, the fitting lines show excellent agreement with measured data points, confirming that the RPA is a good model to express concentration fluctuation for the present miscible polymer system.

In Figure 6, the evaluated interaction parameter values are plotted against the inverse of temperature, $1/T$. The plots are on a straight line fairly well, and it is evidenced the data follow the standard form of $A + B/T$, where A and B are the constants representing the entropic and enthalpic parts of the interaction parameter. By least-squares linear fitting, A and B are obtained as 0.027 and -9.5, respectively. When A is positive and B is negative, the χ changes from positive to negative as temperature increases, indicating that PTMSS/PI blends show LCST-type phase behavior.

Mean-field theory[30] predicts the interaction parameter at spinodal point χ_s as

$$\chi_s = \frac{v_0}{2}\left(\frac{1}{v_A N_A \phi_A} + \frac{1}{v_B N_B \phi_B}\right) \tag{3}$$

When $\phi_A = \sqrt{v_B N_B}/(\sqrt{v_A N_A} + \sqrt{v_B N_B})$ and $\phi_B = \sqrt{v_A N_A}/(\sqrt{v_A N_A} + \sqrt{v_B N_B})$, χ_s gives the critical value χ_c as

$$\chi_c = \frac{v_0}{2}\left(\frac{1}{\sqrt{v_A N_A}} + \frac{1}{\sqrt{v_B N_B}}\right)^2 \tag{4}$$

Substituting the values in Table 2 for v_A, v_B, N_A, and N_B in eq 4, χ_c is calculated as 0.0124, and from the temperature dependence of χ, T_c is calculated as 378 °C, which is much higher than the measured temperature range in this study. If we estimate the critical value for the degree of polymerization at 200 °C, which is a typical high temperature we can reach by the present experiment, 304 is obtained for N_A or N_B. The degree of polymerization for larger molecular weight samples in Table 1 is enough larger than this critical value.

Figure 7 gives the phase diagram of blend-l determined by OM. The open circles show the phase separation temperature for each blend with different volume fractions, and the line is drawn as a guide for the eyes. In the lower region of the line the blends are homogeneous and look transparent as shown in Figure 8a, while they have domain structure over micrometer size and seem turbid in the higher region of the line as shown in Figure 8b, exhibiting a typical phase diagram of lower critical solution temperature (LCST) type. From Figure 7 the critical point is obtained at around 0.4 in terms of PTMSS volume fraction and at around 172 °C.

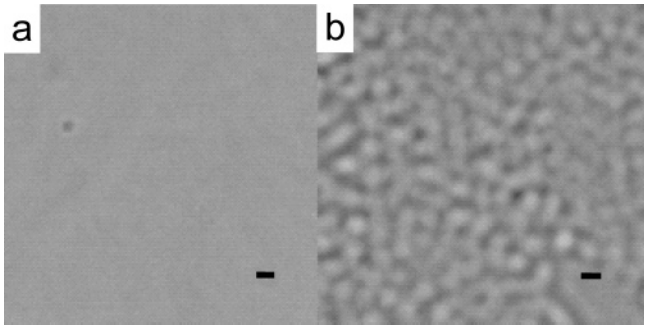

Figure 8. Optical images of blend-l observed at 165 °C (a, left) and at 195 °C (b, right). The volume fraction of PTMSS is 0.4. Bars in each picture correspond to 10 μm.

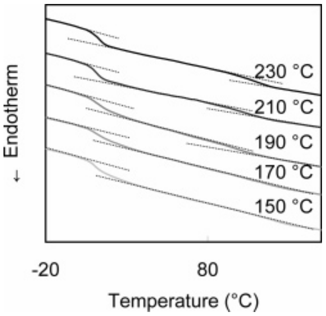

Figure 9. Thermograms of blend-l annealed at various temperatures. The volume fraction of PTMSS is 0.48. Each line is shifted for clarity. Dotted lines are drawn as a guide for the eyes.

T_g's of blend-l with different annealing temperature from 150 to 240 °C were measured by DSC, and their thermograms are shown in Figure 9. A single T_g is observed for the blends annealed at lower temperature than 170 °C, while double T_g is detected for the blends annealed above 190 °C, indicating that the LCST is between 170 and 190 °C.

The SANS profiles of the d-PTMSS/PI blend having larger molecular weight measured at various temperatures are shown in Figure 10, and fitting lines with the RPA are overlaid. Comparing Figure 5 and Figure 10, the sharper increase of intensities at low q region for the latter is evident, reflecting the increase of concentration fluctuation. This is confirmed by the Zimm plot inserted in Figure 10, where the value at $q^2 = 0$ approaches 0 as the temperature increases. The fitting parameters are listed in Table 2, and the evaluated interaction parameter χ's are plotted against the inverse of temperature, $1/T$. As is shown in Figure 11 with open circles and a solid line, the plots are again on a straight line and follow the standard form, which agrees reasonably well with the result of the blend with lower molecular weight shown by small open circle and the dotted line. From this χ and the molecular characteristics in Table 2, the T_c is estimated as 172 °C, which is quite consistent with the results from OM and DSC.

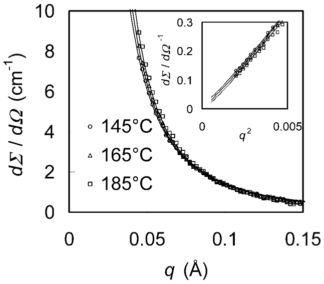

Figure 10. SANS profiles for blend-l heated from 145 °C. The volume fraction of PTMSS is 0.48. The lines are the fitting results with eq 1, using the fitting parameters listed in Table 2. The inlet figure at upper right includes the Zimm plots of the data.

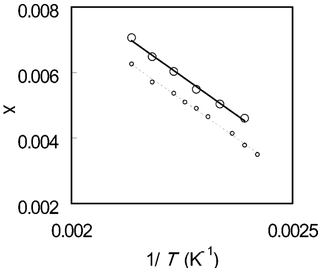

Figure 11. Temperature dependence for χ parameter of blend-l. The solid line is a least-squares linear fitting result. The result of blend-s is overlaid with small open circles and a dotted line.

Table 3. Comparison of Interaction Parameters for Miscible Polymer Systems with LCST

miscible polymer system		A	B (K)	v_0 (nm^3)
d-PS	PVME[a]	0.053	−22	0.124
d-PS	PCHA[b]	0.11	−57	0.198
d-hhPP	PIB[c]	0.025	−10	0.128
d-PTMSS	PI	0.027	−9.5	0.193

[a] PS = polystyrene. PVME = poly(vinyl methyl ether). Cited from ref 8. [b] PCHA = poly(cyclohexyl acrylate). Cited from ref 31. [c] hhPP = head-to-head polypropylene. PIB = polyisobutylene. Cited from ref 32.

Finally, the interaction parameters χ of the PTMSS/PI blend are compared with known miscible polymer blends: polystyrene (PS)/poly(vinyl methyl ether) (PVME),[8] polystyrene (PS)/poly(cyclohexyl acrylate) (PCHA),[31] and head-to-head polypropylene (hhPP)/polyisobutylene (PIB),[32] all having LCST-type phase diagrams. The interaction between PS and PVME was investigated by 2D NMR, and a coupling of phenyl group and ether group was observed.[33] The driving force for miscibility in PS/PCHA was believed to be a weak dipole−induced dipole interaction enhanced by finite rotational states of the segments limited by the bulky cyclohexyl group.[34] The anomalous property of PIB against other polyolefin was explained by lattice cluster theory from the structures of monomers.[35] Their A and B values obtained from the interaction parameters and v_0 employed for analysis by RPA are shown in Table 3. From the comparison one notices that the d-PTMSS/PI blend is similar to the d-hhPP/PIB blend in phase behavior, though the origin of its interaction could be quite different from that of the present polymer blend.

Using 4-trimethylsilylstyrene and isoprene, block copolymers can be synthesized by sequential anionic polymerization,[36] which will be a segregation-tunable microphase-separated system. Structure-controlled PTMSS and PI will give new category of polymer blends with various phase behavior.

Conclusion

The blends of poly(4-trimethylsilylstyrene) (PTMSS) and polyisoprene (PI) were studied by optical microscopy (OM), differential scanning calorimetry (DSC), and small-angle neutron scattering (SANS). We have found that the PTMSS/PI blend is a new miscible polymer system, both component polymers of which can be synthesized anionically. The blends showing homogeneous one phase turns into two phases by heating around 172 °C, which shows the critical point for the lower critical solution temperature (LCST) phase diagram. Below the LCST the blend gives a single glass transition temperature, and the interaction parameter χ is represented as a function of temperature, $0.027 - 9.5/T$, supporting the LCST-type phase behavior.

Acknowledgment. This work was done under the support of COE program entitled “The Creation of Nature-Guided Materials Processing” in the school of Engineering, Nagoya University, which has been assigned as one of the 21st century COE programs. The SANS experiments were performed with the approval of the Institute for Solid State Physics, The University of Tokyo (Proposal 04-4636), at the Japan Atomic Energy Research Institute, Tokai, Japan. M.H. thanks Toyota Central R&D Laboratories, Inc., for support.

References and Notes

(1) *Polymer Blends*; Paul, D. R., Newman, S., Eds.; Academic Press: New York, 1978.
(2) Hammouda, B.; Bauer, B.; Russell, T. P. *Macromolecules* **1994**, *27*, 2357.
(3) Ryu, D. Y.; Park, M. S.; Chae, S. H.; Jang, J.; Kim, J. K.; Russell, T. P. *Macromolecules* **2002**, *35*, 8676.
(4) Russell, T. P.; Karis, T. E.; Gallot, Y.; Mayer, A. M. *Nature (London)* **1994**, *368*, 729.
(5) Ryu, D. Y.; Jeong, U.; Lee, D. H.; Kim, J.; Youn, H. S.; Kim, J. K. *Macromolecules* **2003**, *36*, 2894.
(6) Nishi, T.; Wang, T. T.; Kwei, T. K. *Macromolecules* **1975**, *8*, 227.
(7) Shultz, A. R.; Gendron, B. M. *J. Appl. Polym. Sci.* **1972**, *16*, 461.
(8) Shibayama, M.; Yang, H.; Stein, R.; Han, C. C. *Macromolecules* **1985**, *18*, 2179.
(9) Hirao, A.; Nakahama, S. *Prog. Polym. Sci.* **1992**, *17*, 283.
(10) Khotimskii, V. S.; Filippova, V. G.; Bryantseva, I. S.; Bondar, V. I.; Shantaovich, V. P.; Yampolskii, Y. P. *J. Appl. Polym. Sci.* **2000**, *78*, 1612.
(11) Suzuki, M.; Saigo, K.; Gokan, H.; Ohnishi, Y. *J. Electrochem. Soc.* **1983**, *130*, 1962.
(12) Harada, M.; Suzuki, T.; Ohya, M.; Takano, A.; Matsushita, Y. *Polym. J.* **2004**, *36*, 538.
(13) Seki, M.; Nakano, H.; Yamauchi, S.; Suzuki, J.; Matsushita, Y. *Macromolecules* **1999**, *32*, 3227.
(14) Ito, Y.; Imai, M.; Takahashi, S. *Physica B* **1995**, *213&214*, 889.
(15) Beaucage, G.; Stein, R. S.; Hashimoto, T.; Hasegawa, H. *Macromolecules* **1991**, *24*, 3443.
(16) Sakurai, S.; Jinnai, H.; Hasegawa, H.; Hashimoto, T.; Han, C. C. *Macromolecules* **1991**, *24*, 4839.
(17) Matsuzaki, K.; Uryu, T.; Osada, K.; Kawamura, T. *Macromolecules* **1972**, *5*, 816.
(18) Sato, H.; Tanaka, Y. *J. Polym. Sci., Polym. Chem.* **1979**, *17*, 3551.
(19) Fox, T. G. *Bull. Am. Phys. Soc.* **1965**, *1*, 123.
(20) Lodge, T. P.; McLeish, T. C. B. *Macromolecules* **2000**, *33*, 5278.
(21) Lin, J. L.; Rigby, D.; Roe, R. J. *Macromolecules* **1985**, *18*, 1809.
(22) Bates, F. S.; Wignall, G. D.; Koehler, W. C. *Phys. Rev. Lett.* **1985**, *55*, 2425.
(23) *Scaling Concepts in Polymer Physics*; de Gennes, P. G., Ed.; Cornell University Press: Ithaca, NY, 1978.

(24) *Polymer Handbook,* 4th ed.; Brandrup, J., Immergut, E. H., Grulke, E. A., Eds.; John Wiley & Sons: New York, 2003.

(25) Debye, P. J. *Phys. Colloid Chem.* **1974**, *51*, 18.

(26) Chaumont, P.; Beinert, G.; Herz, J. E.; Rempp, P. *Makromol. Chem.* **1982**, *183*, 1181.

(27) Hashimoto, T.; Nakamura, N.; Shibayama, M.; Izumi, A.; Kawai, H. *J. Macromol. Sci., Phys.* **1980**, *B17*, 389.

(28) Zirkel, A.; Urban, V.; Richter, D.; Fetters, L. J.; Huang, J. S.; Kampmann, R.; Hadjichristidis, N. *Macromolecules* **1992**, *25*, 6148.

(29) Cotton, J. P.; Benoit, H.; Farnoux, B.; Higgins, J.; Jannink, G.; Ober, R.; Picot, C.; des Cloizeaux, J. *Macromolecules* **1974**, *7*, 863.

(30) *Principles of Polymer Chemistry*; Flory, P. J., Ed.; Cornell University Press: Ithaca, NY, 1953.

(31) Schubert, D. W.; Abetz, V.; Stamm, M.; Hack, T.; Siol, W. *Macromolecules* **1995**, *28*, 2519.

(32) Krishnamoorti, R.; Graessley, W. W.; Fetters, L. J.; Garner, R. T.; Lohse, D. J. *Macromolecules* **1995**, *28*, 1252.

(33) Caravatti, P.; Neuenschwander, P.; Ernst, R. R. *Macromolecules* **1986**, *19*, 1889.

(34) Hseih, D. T.; Peifffer, D. G.; Rabeony, M.; Siakali-Kioulafa, E.; Hadjichristtidis, N. *Macromolecules* **1993**, *26*, 4978.

(35) Freed, K. F.; Dudowicz, J. *Macromolecules* **1998**, *31*, 6681.

(36) Harada, M.; Ohya, M.; Suzuki, T.; Kawaguchi, D.; Takano, A.; Matsushita, Y. *J. Polym. Sci., Part B: Polym. Phys.*, in press.

MA048527+